Eero Kolehmainen

PROCESS INTENSIFICATION: FROM OPTIMISED FLOW PATTERNS TO MICROPROCESS TECHNOLOGY

Thesis for the degree of Doctor of Science (Technology) to be presented with due permission for public examination and criticism in the Auditorium 1381 at Lappeenranta University of Technology, Lappeenranta, Finland on the 19th of December, 2008, at noon.

Acta Universitatis
Lappeenrantaensis
330

Supervisor	Professor Ilkka Turunen Department of Chemical Technology Lappeenranta University of Technology Finland
Reviewers	Prof.dr.ir. Henk van den Berg Faculty of Science and Technology University of Twente The Netherlands Professor Laurent Falk, Directeur de Recherche Centre National de la Recherche Scientifique - CNRS Laboratory of Chemical Engineering Science France
Opponent	Professor Laurent Falk, Directeur de Recherche Centre National de la Recherche Scientifique - CNRS Laboratory of Chemical Engineering Science France
Custos	Professor Ilkka Turunen Department of Chemical Technology Lappeenranta University of Technology Finland

ISBN 978-952-214-667-0
ISBN 978-952-214-668-7 (PDF)
ISSN 1456-4491

Lappeenrannan teknillinen yliopisto
Digipaino 2008

ABSTRACT

Eero Kolehmainen
Process intensification: From optimised flow patterns to microprocess technology

Lappeenranta 2008
58 p.
Acta Universitatis Lappeenrantaensis 330
Diss. Lappeenranta University of Technology

ISBN 978-952-214-667-0, ISBN 978-952-214-668-7 (PDF), ISSN 1456-4491

This thesis is focused on process intensification. Several significant problems and applications of this theme are covered.

Process intensification is nowadays one of the most popular trends in chemical engineering and attempts have been made to develop a general, systematic methodology for intensification. This seems, however, to be very difficult, because intensified processes are often based on creativity and novel ideas.

Monolith reactors and microreactors are successful examples of process intensification. They are usually multichannel devices in which a proper feed technique is important for creating even fluid distribution into the channels. Two different feed techniques were tested for monoliths. In the first technique a shower method was implemented by means of perforated plates. The second technique was a dispersion method using static mixers. Both techniques offered stable operation and uniform fluid distribution. The dispersion method enabled a wider operational range in terms of liquid superficial velocity. Using dispersion method, a volumetric gas-liquid mass transfer coefficient of 2 s^{-1} was reached.

Flow patterns play a significant role in terms of the mixing performance of micromixers. Although the geometry of a T-mixer is simple, channel configurations and dimensions had a clear effect on mixing efficiency. The flow in the microchannel was laminar, but the formation of vortices promoted mixing in micro T-mixers. The generation of vortices was dependent on the channel dimensions, configurations and flow rate.

Microreactors offer a high ratio of surface area to volume. Surface forces and interactions between fluids and surfaces are, therefore, often dominant factors. In certain cases, the interactions can be effectively utilised. Different wetting properties of solid materials (PTFE and stainless steel) were applied in the separation of immiscible liquid phases. A micro-scale plate coalescer with hydrophilic and hydrophobic surfaces was used for the continuous separation of organic and aqueous phases. Complete phase separation occurred in less than 20 seconds, whereas the separation time by settling exceeded 30 min.

Fluid flows can be also intensified in suitable conditions. By adding certain additives into turbulent fluid flow, it was possible to reduce friction (drag) by 40 %. Drag reduction decreases frictional pressure drop in pipelines which leads to remarkable energy savings and decreases the size or number of pumping facilities required, e.g., in oil transport pipes.

Process intensification enables operation often under more optimal conditions. The consequent cost savings from reduced use of raw materials and reduced waste lead to greater economic benefits in processing.

Keywords: Microreactors; microprocess; monoliths; microseparation; micromixer; process intensification, drag reduction

UDC 66.011 : 66.023.2

ACKNOWLEDGEMENTS

The research work for this thesis has been carried out at Lappeenranta University of Technology in the Laboratory of Product and Process Development and also partly in Neste Engineering Oy.

I express my thanks to my supervisor Professor Ilkka Turunen for his advice and giving me the opportunity to research and study this very interesting area.

I thank the reviewers, Professor Henk van den Berg and Professor Laurent Falk for their valuable comments on the content of my work.

I thank Peter Jones for assistance with the language of this thesis.

The Finnish Funding Agency for Technology and Innovation (TEKES) and The Graduate School of Chemical Engineering (GSCE) are gratefully acknowledged for funding this work.

Many people have helped me with the research work for this thesis. I wish to mention some of them by name. I would like to thank Timo Haakana M.Sc. for his close co-operation, friendship and ensuring a pleasant atmosphere during this project, both at the university and outside. I express my thanks also to Benguang Rong D.Sc. (Tech.) for valuable discussion and advice. Azita Soleymani D.Sc. (Tech.) is acknowledged for her efficient work. I also want to thank all the other co-authors in my publications as well as the personnel of the Laboratory of Product and Process Development. When I have needed technical support in my work, Markku Maijanen, Markku Korhola and Ari Ryhänen have been very helpful and they deserve my thanks. I thank also Juha Väyrynen M.Sc from Joensuun Tiedepuisto Oy Imtec for constructing some of the microstructured equipment.

Warmest thanks go to the people closest to me, my parents and brothers. Finally, I owe my deepest gratitude to Kati, who has been very kind and patient, supporting me and taking care of me during the most demanding stages of this project.

Lappeenranta, December 2008

Eero Kolehmainen

TABLE OF CONTENTS

LIST OF PUBLICATIONS

This thesis is based on the following publications, which are referred in the text by Roman numbers I-VII.

I. Rong, B-G., Kolehmainen, E., Turunen, I., Hurme, M. (2004). Phenomena-based methodology for process intensification, *Computer-Aided Chemical Engineering, ESCAPE-14*, **18**, A. Barbosa-Povoa, H. Matos (Eds.), Elsevier Science, pp. 481-486.

II. Haakana, T., Kolehmainen, E., Turunen, I., Mikkola, J-P., Salmi, T. (2004). The development of monolith reactors: general strategy with a case study, *Chemical Engineering Science*, **59**, pp. 5629-5635.

III. Haakana, T., Kolehmainen, E., Turunen, I. (2005). Comparison of Flow Patterns and Gas-Liquid Distribution Techniques in Monolith Reactors, *Proceedings of the 7th World Congress of Chemical Engineering*, Glasgow Scotland, 10-14 July 2005, 10 pages.

IV. Soleymani, A., Kolehmainen, E., Turunen, I. (2008). Numerical and experimental investigations of liquid mixing in T-type micromixers, *Chemical Engineering Journal*, **135S**, pp. S219-S228.

V. Kolehmainen, E., Turunen, I. (2007). Micro-scale liquid-liquid separation in a plate-type coalescer, *Chemical Engineering and Processing*, **46**, pp. 834-839.

VI. Koskinen, J., Manninen, M., Pättikangas, T., Alopaeus, V., Keskinen, K.I., Kolehmainen, E. (2004). Measurements and CFD Modeling of Drag-Reduction Effects, *SPE Production & Facilities*, **19**, pp. 142-151.

VII. Kolehmainen, E., Oinas, P., Turunen, I. (2005). Intensified processes for continuous production of fine and specialty chemicals, *Sustainable (Bio)Chemical Process Technology Incorporating the 6th International Conference on Process Intensification*, P. Jansens et al. (Ed.), Delft, The Netherlands, 27-29 September 2005, BHR Group, pp. 253-262.

OTHER RELATED PUBLICATIONS

Rong, B-G., Kolehmainen, E., Turunen, I. (2008). Methodology of conceptual process synthesis for process intensification, *Computer-Aided Chemical Engineering, ESCAPE-18*, **25**, B. Braunschweig, X. Joulia (Eds.), Elsevier, The Netherlands, pp. 283-288.

AUTHOR'S CONTRIBUTION IN THE PUBLICATIONS

For I, the author participated in method development, concluding and writing the paper. For II and III, the author carried out the experiments with co-authors and participated in the evaluation of the results and conclusions. For IV, the author was responsible of the experimental part and participated in concluding and writing the paper. For V, the author had a major role in the experimentation, conclusions and he also wrote the paper. For VI and VII the author participated in all the steps and had a major role in calculations.

LIST OF SYMBOLS

A_{cr}	cross-sectional area	, m^2
a	specific area	, 1/m
a_i	experimental parameter value, in Eq. (4)	, -
C	concentration of drag reducing polymer	, ppm
c_i	concentration of component i	, mol/l
$c_{i,sat}$	saturation concentration of component i	, mol/l
D	diameter of cylinder	, m
D_i	diffusion coefficient	, m^2/s
DR_{max}	maximum drag reduction effect	, %
DR-%	drag reduction effect	, %
DR-%$_0$	initial drag reduction effect	, %
E	separation efficiency	, %
k_la	mass transfer coefficient	, 1/s
L	length	, m
M	apparent molar mass	, g/mol
M_f	final molar mass	, g/mol
M_0	initial molar mass	, g/mol
n	rotation speed	, 1/s
Δp_{DRA}	pressure drop with DRA	, Pa
Δp_0	pressure drop without DRA	, Pa
T_{DRA}	torque with DRA	, Nm
T_0	torque without DRA	, Nm
t	time	, s
u_i	superficial velocity of component i	, m/s
u_{tot}	total superficial velocity	, m/s
V_i	volume	, m^3
$\dot{V}_i$	volumetric flow rate	, m^3/s
x_i	mass fraction	, -

Greek symbols

ε_i	hold-up	, -
γ_i	activity function	, -
ν	kinematic viscosity	, m^2/s
τ	time constant of polymer decay	, s

Subscripts

g	gas
l	liquid
m	monolith

Dimensionless number

$\mathrm{Re} = \frac{nD^2}{\nu}$	Reynolds number for rotating devices

Chemicals and abbreviations

CH_3OH	methanol
$(CH_3)_2CO$	acetone
HCl	hydrochloric acid
H_2O	water
$H_3CC(OCH_3)_2CH_3$	2,2-dimethoxypropane
NaCl	sodium chloride
NaOH	sodium hydroxide
N_2	nitrogen
O_2	oxygen
CFD	computational fluid dynamics
DRA	drag reducing agent
DR	drag reduction

1 INTRODUCTION

1.1 Background

Chemical engineering faces many challenges nowadays and is having to adjust to changing circumstances. Environmental aspects are very important and the development of environmentally benign processes is fundamental. Saving resources and producing more from fewer resources is a central goal in future chemical processing. Globalisation also poses challenges. Savings in raw material consumption and investments are required at a time of limited profit margins. All these aspects are pushing chemical and process engineering towards intensification.

1.2 Process intensification

The concept of process intensification was first proposed in the 1980's by Ramshaw (1983). He defined it as design strategy to make dramatic changes in plant sizes by several orders of magnitude. The size reductions in chemical plants may be results from the decreased size of processing units or a decreased number of processing units. Ramshaw (1983) also presented the concept of the HIGEE gas-liquid contactor, where centrifugal force is used to intensify mass transfer in packed bed.

The definition of process intensification was extended by Stankiewicz and Moulijn (2000). They produced a definition that process intensification means novel equipment, processing techniques and process development methods that can offer substantial improvements in biochemical and chemical processing in terms of energy consumption, waste generation, plant sizes, etc. According to their definition, process intensification has two areas: equipment and methods, as shown in Figure 1.

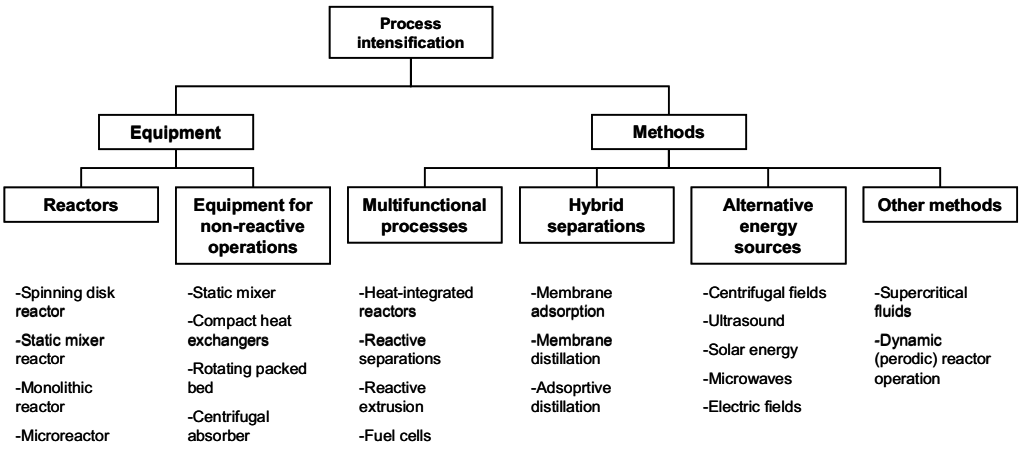

Figure 1. Areas of process intensification.

1.2.1 Design philosophy in process intensification

The goal of process intensification is to reduce plant costs and to design cost effective processes. This may be conducted by making improvements in existing technologies but, an essential aspect of process intensification is also the development of new technology. The design philosophy in process intensification is to design a process which has chemical kinetics as its only limitation. This means that all other processing limitations such as mass transfer, heat transfer and hydrodynamics are eliminated, as shown in Figure 2 (Bakker et al., 2001).

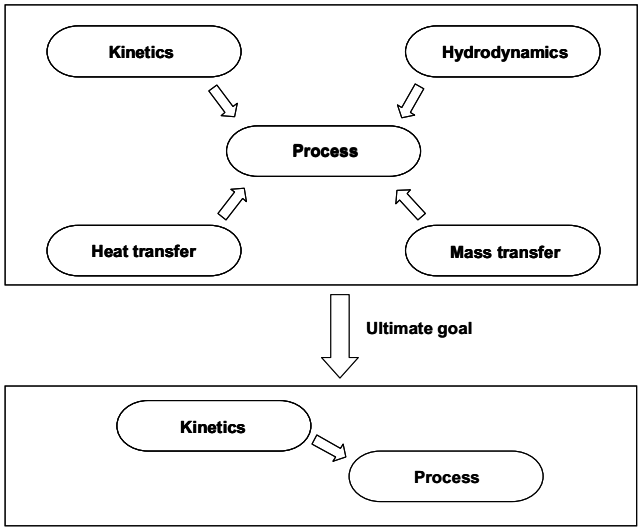

Figure 2. Design philosophy in process intensification. Elimination of extra limitations.

1.3 Microreactor technology

Microreactor technology represents process intensification at its extreme. Developments in manufacturing technology during the last 20 years have enabled the production of miniature components for chemical reactor technology. These components are often called microreactors.

Microreactors can be generally defined as microstructured devices designed for chemical engineering purposes such as reactions, heat and mass transfer. As a result of active research and development in the field, microscale processing units such as micromixers, micro heat exchangers and reaction modules are commercially available. The microscale structures are usually applied inside the reactors; the whole microreactor system may have outer dimensions on a macroscale.

Microreactor components have been developed and applied for liquid, liquid-liquid, gas, gas-liquid and gas-liquid-solid phase processes. They have many advantages as research tools and on a production scale. The dimensions of channels in microreactors are typically in submillimetre range. Production scale applications contain a large number of parallel small channels. The small channel sizes mean a high ratio of surface area to volume, which leads to efficient heat and mass transfer characteristics. In highly exothermic reactions, elimination of local hot-spots and runaways is then possible and fast mixing can be achieved. These aspects make microreactor technology suitable for very fast and highly exothermic reactions, where conditions have clear effects, for example, on reaction selectivity (Hessel et al., 2004).

Other advantages of microreactor technology are summarised below:

- Short residence times are possible
- Continuous production is possible due to high heat and mass transfer rates
- Potential for rapid process development by parallelisation of units
- Inherent safety due to small internal volumes of units
- Modularity brings flexibility

On the other hand, there are certain challenges for microreactors. Due to the small internal dimensions, the microstructured components are vulnerable to solid particles. The process development of microreactors from laboratory scale to production scale is to be performed by

number-up principle instead of traditional scale-up. The number-up concept is based on the repetition of single units when phenomena remain constant during process development. This leads to large number of parallel channels. In multichannel devices, the achievement of even fluid distribution into channels is a real challenge. The investment cost of microreactors can be assumed to be high because a lot of construction material is needed for small internal volumes.

1.4 Scope of the work

In microreactor and microprocess technology, process development is principally based on number-up principle, that is, repetition of a channel or a unit. It is a straightforward approach and eliminates errors originating from scale differences during process development. However, other problems appear such as fluid distribution problems. It is not easy to distribute fluid evenly in many parallel channels. Proper chemical feeding is an important aspect in chemical engineering. In addition, in the case of many parallel channels, the manufacturing costs of a microreactor may become high. In order to make microprocess technology feasible for large scale operations, the above mentioned challenges have to be met. Reliable and proper chemical feeding and a non-complex structure of devices create a successful basis for reliable process development and intensification. The objective of this thesis is to show the importance of flow patterns, chemical feeding and simple and efficient structures in the intensification of chemical and transport processes. By combining and utilising creatively hydrodynamics, structures, materials and conditions, it is possible to develop intensified process units.

1.5 Outline

This thesis summarises the results from the publications I-VII. The main results from publication I are presented in chapter 2.1. The results from publications II and III are presented in chapter 3.1.1. The results from publication IV are summarised in chapters 3.2.1 and 3.2.2. The main results from publication V are presented in chapters 3.3.1 and 3.3.2. The main results from publication VI are summarised in chapter 4.1 and the main results from publication VII are presented in chapter 5.

2 PROCESS INTENSIFICATION METHODOLOGIES

A systematic procedure of process intensification for creating optimal designs for chemical processes either by developing existing technology or creating new designs has received little consideration in literature. Two general methods are explained here. In addition, an alternative method was developed for a systematic methodology for process intensification, chapter 2.1.

Green et al. (1998) describe a methodology, in which both business and process drivers are the starting point. All necessary information concerning the process is first collected. The information is used to recognise certain process intensification blockers and limiting steps in the process. After generating design concepts, the feasibility of process intensification is assessed. The further steps of the methodology describe the selection, evaluation and comparison of the concepts for process intensification. A schematic overview of the process intensification methodology by Green et al. is shown in Figure 3. In this method, the generation of design concepts for process intensification is not considered.

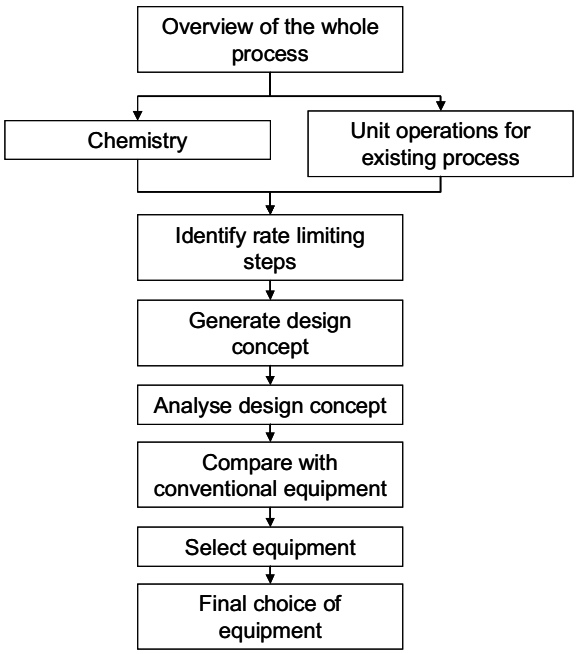

Figure 3. Process intensification methodology by Green et al. (1998).

Bakker et al. (2001) presented the general methodology, which has been applied at DSM company. Multidisciplinary teams are involved in the work. The current chemistry of the process is the starting point and the only limiting factor in the methodology. Possibilities for radical improvements to existing processes are scouted. After brainstorming sessions, a general process design and cost estimates are created. The methodology is general producing general designs leaving final details of process design for further stages. The methodology is presented schematically in Figure 4.

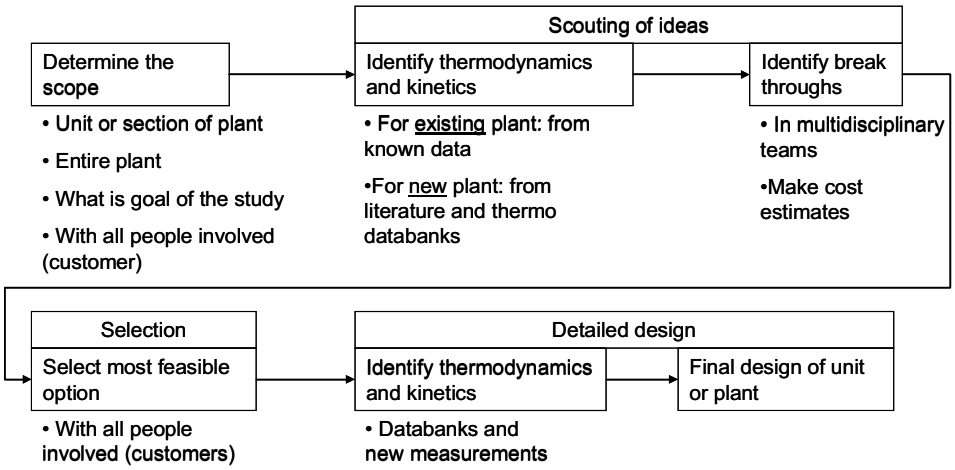

Figure 4. Process intensification methodology by Bakker et al. (2001).

2.1 Phenomena-based methodology

In this thesis, a phenomena based methodology for process intensification was developed based on examination of chemical and physical phenomena in the process. Phenomena are defined in this study as basic physical and chemical changes in the process and interactions between different substances.

2.1.1 Procedure of phenomena-based methodology

The phenomena-based methodology consists of several steps. The approach is presented in Figure 5.

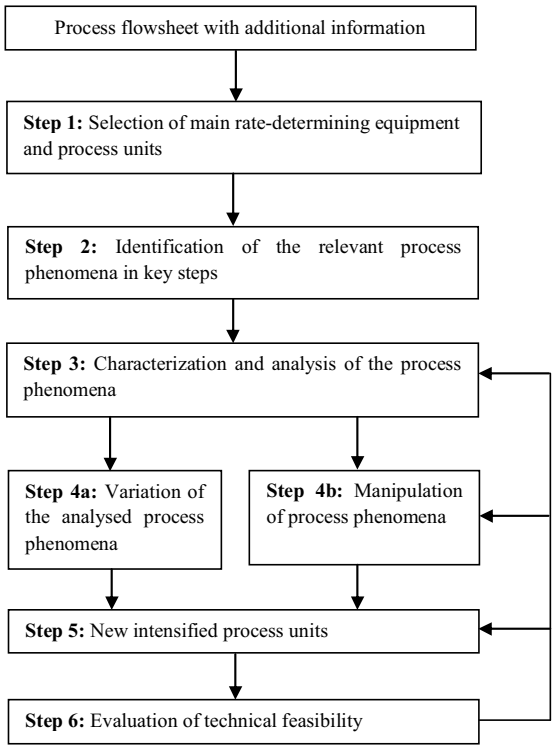

Figure 5. Steps of phenomena-based methodology for process intensification.

First, a potential rate-determining step in the process is selected for analysis. The relevant phenomena in the step are then identified. In the next step, the phenomena are characterised based on the attributes in five categories presented in Table I. The characterisation based on the attributes is applied to each of identified phenomenon.

TABLE I Categories and attributes for characterisation of the process phenomena.

Phases+	Changes of variables	Energy source	Geometry*	Surface material
L/G	Temperature	Gravity	Geometry (1)	Metal
L/S	Pressure	Centrifugal	(*Equipment*)	Ceramic
S/G	Concentration	Microwave	Tank	Plastics
L	Velocity	Ultrasound	Column	Chemical
G	Density	Electromagnetic	Tube	surface (act.)
S	Viscocity	Motor	Nonconventional	
S/L/G		Heat transfer fluid	Geometry (2)	
L/L		Magnetic field	(*Internals)*	
L/L/G		Reaction	Geometry (3)	
L/L/S			(*Surfaces*)	

+ L:liquid, G:gas, S:solid
*Geometry (2): packings, plates, films, spray, uniform, fiber, specific structures
Geometry (3): even, rough, porous

The ideas for new equipment are searched systematically by variation of the process phenomena. The variation is performed by systematically trying and testing different combinations of the attributes listed in Table I. Another approach to get more ideas and concepts for substantial process improvements is to manipulate process phenomena following the principles shown in Table II.

TABLE II General principles for manipulation of the process phenomena.

	Principles	Examples
1	*Enhance* a favorable phenomenon	Enhance an oxidation reaction by using oxygen instead of air
2	*Attenuate* an unfavorable phenomenon	Decrease side-reactions by shortening residence time
3	*Eliminate* a phenomenon	Eliminate an azeotropic behavior by adding a solvent in a distillation system
4	*Combine* several process phenomena	Combine reaction and distillation into a reactive distillation
5	*Separate* phenomena	External catalyst packages in reactive distillation
6	*Mitigate* the effect of a phenomenon by combining it with another	Eliminate reaction equilibrium limit by removing desired product immediately
7	*Create* a new phenomenon	Create a new phase interface for mass transfer

2.1.2 Interpreting the case study using the phenomena-based methodology

A hydrogen peroxide production process is used as a case study for the phenomena-based methodology. The goal is to test if the results of process intensification in the hydrogen peroxide process (Turunen, 1997) can be interpreted using this methodology.

2.1.2.1 Identification and analysis of phenomena

Hydrogen peroxide is produced by means of an organic autooxidation process. A short description of the hydrogen peroxide production process is given in publication I. The main process phenomena in the hydrogen peroxide production process are the reactions and mass transfer. Hydrogenation, oxidation and extraction represent the main steps in the process. The hydrogenation is a gas-liquid reaction in the presence of a suspended solid catalyst. The oxidation is a noncatalytic gas-liquid reaction carried out in a bubble or packed column. The oxidation column is the largest equipment in the conventional production technology. The main phenomena in the oxidation step are:

- gas-liquid mass transfer (dissolving of oxygen into the working solution)
- oxidation reaction producing hydrogen peroxide

The extraction of the hydrogen peroxide from the working solution is usually carried out in a sieve-plate column, which is the second largest equipment in the process. The main phenomenon in the extraction is the liquid-liquid mass transfer of hydrogen peroxide from the organic working solution into the aqueous phase.

2.1.2.2 Phenomena manipulation and principles for process intensification

Depending on the conditions in the oxidation stage, either mass transfer of oxygen into the working solution or the oxidation reaction itself represents the main process phenomena. These phenomena can be enhanced by using oxygen instead of air according to Principle 1 in Table II. In order to increase the mass transfer efficiency and decrease the size of equipment, the reactor type in the oxidation stage is changed from conventional a column to tubular reactor with static mixers. In the intensification of hydrogenation, the suspension catalyst was replaced by a specific fixed bed catalyst structure. The main achievement was the elimination catalyst filtration. These results could be interpreted by applying the variation approach (Step 4a).

The presented phenomena-based methodology facilitates systematic idea generation for process intensification and aims to find new intensified process options for substantial improvement in process performance. The new ideas and concepts need further analysis and

evaluation in a conventional way. The case study indicates that the intensification results of hydrogen peroxide process can be interpreted with this method.

3 EQUIPMENT FOR PROCESS INTENSIFICATION

The area of process intensification consists of equipment and methods (Figure 1). In this thesis, the focus is on the intensifying equipment, especially monoliths and microprocess components. According to the design philosophy of process intensification, hydrodynamic and mass transfer limitations should be eliminated in the design of the intensified processes. The feeding of chemicals into a reactor and efficient mass transfer in the reactor have great importance from the viewpoint of reactor performance, the importance of suitable flow patterns is, therefore, emphasised in this thesis.

3.1 Monolithic reactors

Monolith structures have been applied in catalytic reactions. The major application field is catalytic gas phase conversions, e.g., in automotive exhaust treatment and flue gas treatment of power plants. Catalytic gas-liquid phase operation is also an attractive field for monoliths. A monolith structure consists of many narrow parallel channels separated by a channel wall. Different channel geometries, e.g., square, triangular, hexagonal or sinusoidal, have been used. The construction material of monoliths is ceramics or metals (Edvinsson and Cybulski, 1995; Cybulski et al., 1999; Roy et al., 2004).

There are number of features, which make monoliths beneficial in chemical engineering. Monoliths act as a regular catalyst structure, so there is no need for specific separation of the catalyst and product in the processing. Monoliths can provide a high surface area per reactor volume, high interfacial mass transfer rates and short diffusion lengths in the catalyst. These features are important especially in processes where mass transfer resistances play a significant role in terms of reaction yield and selectivity. Low pressure drop along channels is also characteristic for monoliths (Kreutzer et al., 2001; Heiszwolf et al., 2001).

Monoliths suffer from shortcomings relating to the flow distribution. In gas-liquid processes, it is a clear challenge to achieve even flow distribution into the parallel channels. Uneven flow distribution leads to unstable gas and liquid flow in the channels that has a negative effect on reactor performance (Heibel et al., 2001). Other disadvantages of monoliths are difficult catalyst regeneration and inefficient heat transfer, especially in ceramic monoliths.

Heat transfer has to take place by conduction since the channel walls prevent radial dispersion.

In order to distribute liquid and gas properly into the monolith, various feed techniques have been applied such as the perforated plate (Irandoust, 1989), thin monolith slice (Satterfield, 1977), glass frit (Crynes, 1995) and liquid-driver ejector (Broekhuis, 2001). Several methods have been used to study flow distribution in monoliths. The methods can be categorised as direct and indirect. In indirect methods, a conclusion on flow distribution is made based on the performance of the monolith in terms of variables such as pressure drop and mass transfer measurements. Bercic and Pintar (1997) observed that a volumetric gas-liquid mass transfer coefficient can be expressed as a function of the total superficial velocity and liquid slug length. They carried out experiments in a single capillary and proposed the following correlation between volumetric mass transfer coefficient and flow characteristics:

$$k_l a = \frac{0.111 u_{tot}}{L_l^{0.57}} \qquad (1)$$

In direct methods, specific measurements are used to study flow distribution. Tomographic methods (Reinecke and Mewes, 1996 and 1997) and magnetic resonance imaging (MRI) (Heibel et at., 2001; Gladden et al., 2003; Mantle and Sederman, 2003) are suitable non-invasive methods for quantitative analysis of phase distribution in multiphase reactors.

3.1.1 Study of flow phenomena

In this thesis, feed techniques and gas-liquid mass transfer in the monolith reactor were under consideration. Flow patterns and mass transfer were studied in ceramic (cordierite) monolith elements having 400 cells per square inch and channel diameter of 1.08 mm. In the study, two principles for feed techniques were applied: a shower method using a perforated plate and a gas-liquid dispersion method using Sulzer-type SMX- and SMV-static mixers. Concurrent downward and upward operation modes were tested and comparison between the modes was based on the flow phenomena and the volumetric gas-liquid mass transfer coefficient. In the case of the perforated plate, only concurrent downward operation mode was used. The range

of liquid superficial velocity with the shower method was 0.09-0.16 m/s and with the dispersion method 0.16-0.42 m/s. The maximum gas superficial velocity was 0.26 m/s.

3.1.1.1 Experimental set-ups for flow patterns and gas-liquid mass transfer

A visual method was first developed to study flow patterns in the monolith section. A monolith block was cut into a thin rectangular slice (150 mm x 80 mm x 2 mm) through which light was emitted. Both photo images and video recordings were taken. The obtained visual data was used to identify gas and liquid flows, bubble lengths, slug lengths and phase distribution in the monolith channels. This information was utilised in determining the gas-liquid interfacial area, in design, and in comparison of gas-liquid feed techniques. More detailed information on experiments is given in publications II and III. The experimental set-up of the method is shown in Figure 6.

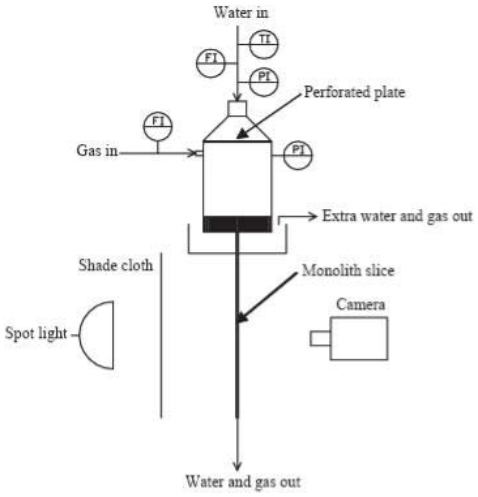

Figure 6. Experimental set-up to study flow phenomena in a monolith structure.

In the study on gas-liquid mass transfer, the diameter of the monolith section and the static mixer was 80 mm. The total length of the monolith unit was 610 mm. More detailed information on experiments is given in publications II and III. The configurations used are shown in Figure 7.

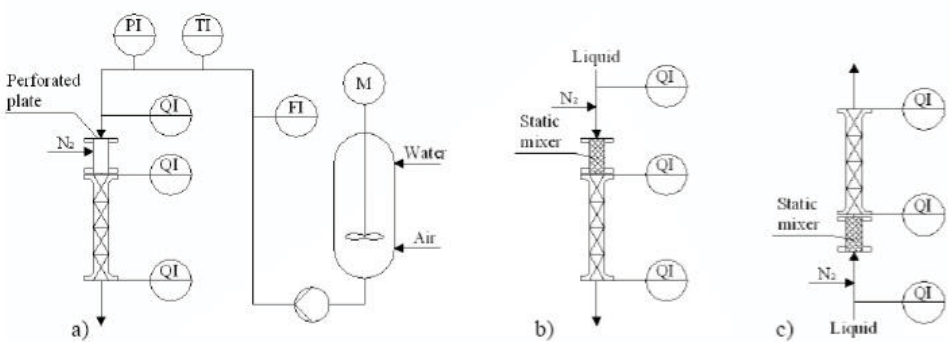

Figure 7. Experimental set-ups to study gas-liquid mass transfer: a) the overall set-up using the shower method with perforated plate, b) downward dispersion method with static mixer and c) upward dispersion method with static mixer.

In the experiments, water was first saturated by oxygen and then fed through the distribution device into the monolith section. In the shower method, nitrogen was fed just below the perforated plate above the monolith section. In the dispersion mode, nitrogen was fed to the centreline of the feed tube just in front of the static mixer. Oxygen was transferred from the liquid to gas phase and nitrogen from the gas phase to liquid phase in the monolith section. Oxygen concentration in liquid was analysed in the inlet and in the outlet of the monolith.

3.1.1.2 Results

The average lengths of liquid slugs in the monolith channels were studied as a function of gas and liquid superficial velocities by using the above mentioned feed techniques. The effect of superficial velocities and feed techniques on the average slug length is shown in Figure 8. Increasing the gas flow rate significantly decreases the average liquid slug length. In upward operation mode, the average lengths of liquid slug are smaller than in downward mode.

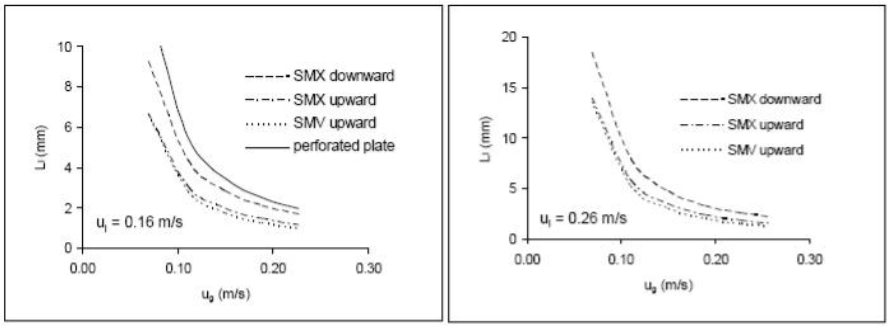

Figure 8. Effect of gas superficial velocity and feed technique on average slug lengths at different liquid superficial velocities.

In order to estimate the volumetric gas-liquid mass transfer coefficient for the system, material balances for oxygen and nitrogen in liquid phase were derived and they are presented in the following Equations (2) and (3),

$$\frac{dc_{O_2}}{dL} = k_l a\left(c_{O_2,sat} - c_{O_2}\right) / \dot{V}_l / A_{cr}\left(1-\varepsilon_m\right)\left(1-\varepsilon_g\right) \tag{2}$$

$$\frac{dc_{N_2}}{dL} = k_l a \frac{D_{N_2}}{D_{O_2}}\left(c_{N_2,sat} - c_{N_2}\right) / \dot{V}_l / A_{cr}\left(1-\varepsilon_m\right)\left(1-\varepsilon_g\right) \tag{3}$$

The volumetric gas-liquid mass transfer coefficient was expressed based on empirical correlation as a function of gas and liquid superficial velocity,

$$k_l a = a_1 u_l^{a_2} u_g^{a_3} \tag{4}$$

The parameters a_1, a_2 and a_3 were estimated using ModEst-software (Haario et al., 1994). The estimated parameters for different feed techniques are presented in Table III.

TABLE III Estimated parameters for gas-liquid mass transfer coefficient with different distributor types.

Distributor type	Flow direction	a_1	a_2	a_3	R_2 (%)
Perforated plate	downward	11.47	-0.050	1.397	94.0
SMX	downward	14.33	0.074	1.334	94.0
SMX	upward	16.46	0.014	1.356	94.3
SMV	downward	16.53	0.410	1.204	86.4
SMV	upward	22.17	0.041	1.448	96.0

Comparison of the different feed techniques based on the volumetric gas-liquid mass transfer coefficient is shown in Figure 9 a)-c). The parameter values in Table III are near to each other indicating similar performances for the different feed techniques in the downward mode. Therefore, it can be concluded that flow patterns in the monolith channels have to be rather equal. This can be also concluded from Equation (1), since similar values of mass transfer coefficient indicate approximately similar average slug lengths. The mass transfer efficiency in downward flow is similar when using perforated plate and static mixers, as can be seen from Figure 9 a) and 9 b). Observable enhancement can be found in mass transfer efficiency when a SMX static mixer is used in upward operation mode instead of downward mode as

illustrated in Figure 9 c). Average lengths of liquid slugs are smaller in upward mode than in downward mode (Figure 8). From the operational point of view, using static mixers eliminates the risk of clogging of the distributor and offers a wider operation range than the perforated plate. The risk of clogging obviously exists for the perforated plates.

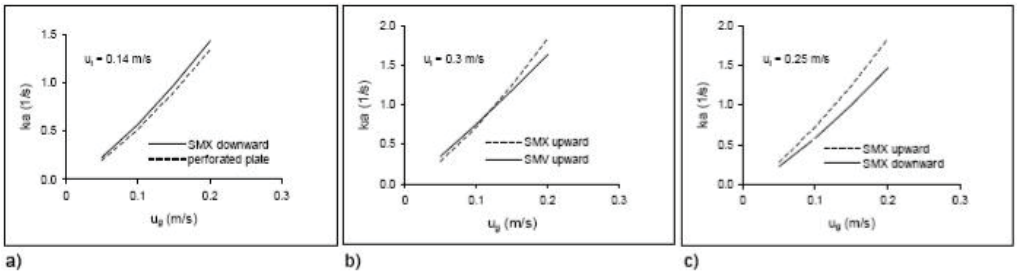

Figure 9. Comparison of the different gas-liquid distribution techniques and their effect on the gas-liquid mass transfer coefficient.

Reliability and identifiability of parameters were studied by deriving contour plots for constant R^2-values and for values of the R^2-objective function when parameter values (a_1, a_2 and a_3) were varied within the certain intervals. This method reveals whether there is a strong intercorrelation between the estimated parameters. The objective function profiles and contour plots are shown in Figure 10, indicating relatively good identification and reliability of the estimated parameters.

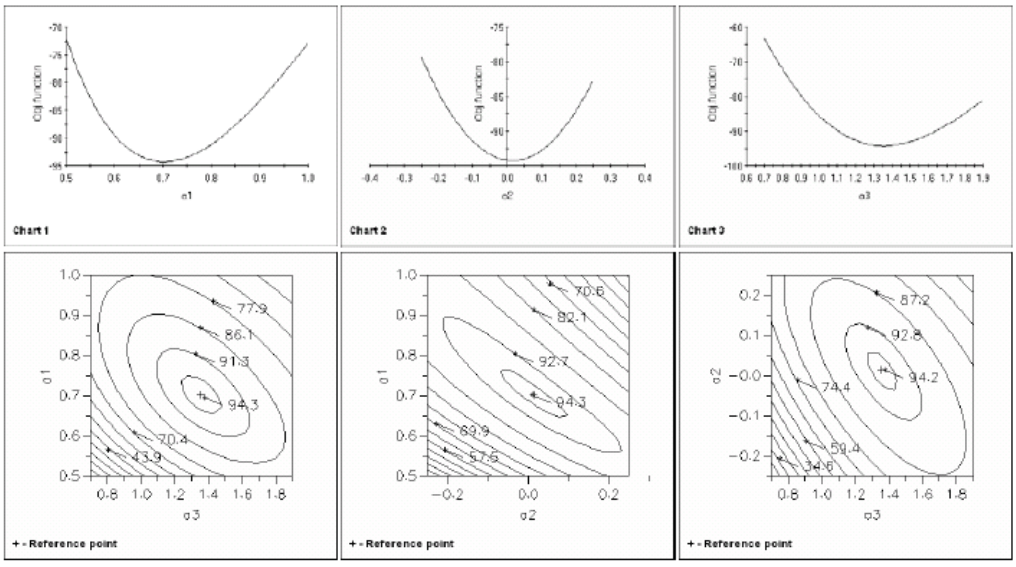

Figure 10. Identifiability of the estimated parameters for the case of the Sulzer-type SMX-static mixer in upward operation mode.

3.2 Microstructured mixers

Mixing and chemical feeding are often dominant factors in chemical reactor performance. It is assumed that continuous in-line mixing will become more and more attractive compared to stirred-tank mixing in future (Kresta et al., 2004). Furthermore, there are drivers, which favour the use of microstructured mixers in mixing tasks. Small internal volumes provide short residence times which is a requirement when operating with fast reactions. Small internal volume also means inherently safe operation. (Hessel et al., 2005b). Microstructured mixers are applicable for a wide operational range from analytical applications to production scale. (Bayer, 2003)

Several types of microstructured mixers have been developed and applied during recent years (Hessel et al., 2005a). In this thesis, micromixers utilising bi- and multilamination principles in liquid mixing are under consideration. In bilamination mixers, the fluids entering the mixing channel form two layers at the beginning of the mixing channel. An example of a bilamination mixer is a mixing T (T-mixer). In multilamination mixers, several fluid layers are formed at the beginning of the mixing channel. The division of the fluid into several layers takes place by means of specific structures.

T-mixers (and Y-mixers) represent the simplest in-line mixer type. Numerous studies, both numerical and experimental, show that even if the geometry of T-type mixers is simple, the hydrodynamic phenomena are rather complex. Different flow patterns in the mixer greatly affect the mixing performance. The fluid flow in microchannels is laminar. However, formation of vortices causes convection that significantly promotes mixing (Engler et al., 2004; Wong et al., 2004; Bothe et al., 2006; Hoffman et al., 2006).

On a laboratory scale, multilamination micromixers (Ehrfeld et al., 1999) have been widely used devices in microprocesses. They enable efficient mixing in the laminar regime. In multilamination mixers, the main feed streams are first divided into several layers (multilamellae), after which they are fed into contact in parallel. The thickness of a single fluid layer is usually of the order of tens of micrometers (40 μm in Figure 11 b). Decrease in the thickness of the fluid layers, makes the diffusion length shorter and the diffusion faster. Figure 11 shows an example of the structure of a micromixer, the *Slit Interdigital Micro Mixer* (IMM, Institut für Mikrotechnik Mainz). The division of the feed streams occurs in the

mixing element shown in Figure 11 b). After division, the fluid layers, which are called multilamellae, are fed through the discharge slit to the outlet shown in Figure 11 a).

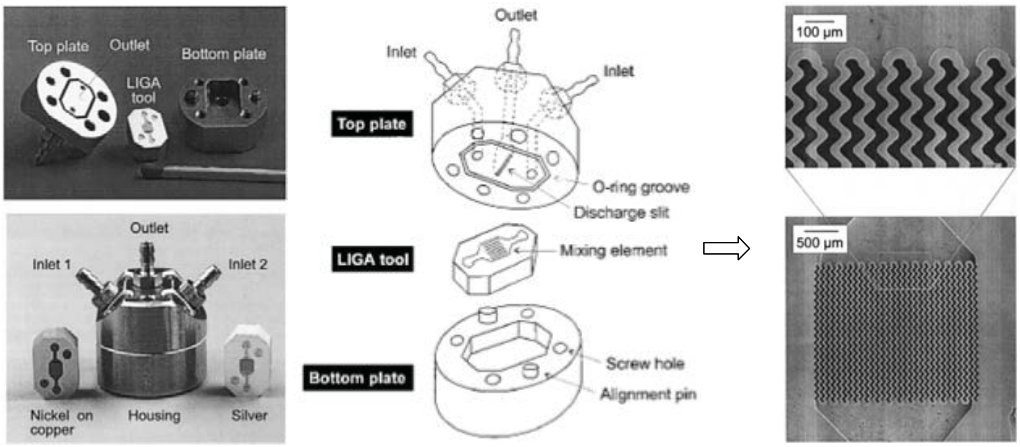

Figure 11. Slit Interdigital Micro Mixer (IMM, Institut für Mikrotechnik Mainz). a) Pieces of the micromixer. b) magnification of the mixing element, where alternating arrangement for fluid layers takes place (interdigital feed) (Ehrfeld et al., 1999).

Figure 12 illustrates multilamellae flow arrangement. The feed system is called an interdigital feed. It has been reported that different flow patterns exist in the multilamination mixers. The thicknesses of lamellae decrease when flow is focused in a borehole and zones with recirculation are generated (Hessel et al. 2003).

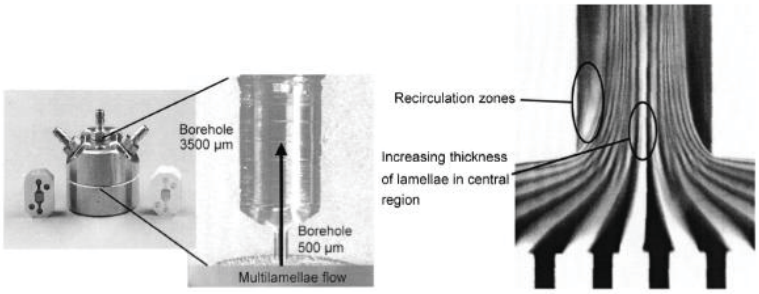

Figure 12. Multilamination flow arrangement in the Slit Interdigital Micro Mixer. Compression of multilamellae and formation of vortices (Hessel et al., 2003).

3.2.1 Numerical simulations of the effects of design variables

The aim of this study was to design efficient micro T-mixers. The effect of various design parameters on mixing efficiency was studied by computational fluid dynamics (CFD).

Numerical simulations revealed that vortices in T-mixers greatly affect the mixing efficiency. Formation of vortices depends significantly on geometrical parameters such as channel dimensions, aspect ratio (channel height/channel width) and flow rates in T-mixers. Detailed information on the simulations is given in publication IV.

In the simulations, variation of flow rate resulted in changes in flow patterns in the mixer. When the flow rate (Reynolds number) was increased, the flow patterns changed from a *stratified* flow pattern to the *vortex* pattern and further to *engulfment* flow patterns. Figures 13 a) c) and e) illustrate the path lines at the entrance of the mixing channels for stratified, vortex and engulfment regimes, respectively. The streamlines of the components are shown in Figure 13 b) d) and f) for stratified, vortex and engulfment regimes, respectively.

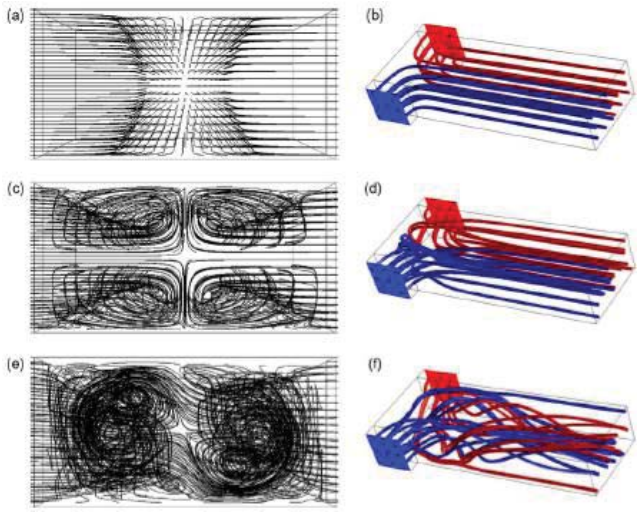

Figure 13. Path lines and streamlines of the components in: a)-b) stratified flow regime, c)-d) vortex regime, e)-f) engulfment regime. Width of the mixing channel is 600 µm and height is 300 µm.

In the stratified flow regime, the mixing is based only on the molecular diffusion, since streamlines of the components are situated side by side in the mixer channel. In the vortex and engulfment regimes, the symmetry of streamlines is destroyed. The vorticity increases the mass transfer area between components and decreases the diffusion lengths further, mixing efficiency is therefore, improved at higher flow rates. An increased number of vortices makes the role of convection in mixing more significant.

Aspect ratio is defined as the ratio of channel height to channel width. Figures 14 a), b), c) and d) illustrate the path lines at the entrance of the mixing channels for aspect ratios of 0.03, 0.42, 0.58 and 0.83, respectively. The streamlines of the components for the aspect ratios of 0.03, 0.42, 0.58 and 0.83 are shown in Figure 14 e), f), g) and h), respectively. Numerical results indicated that increase in aspect ratio changes the flow pattern in the mixing channel.

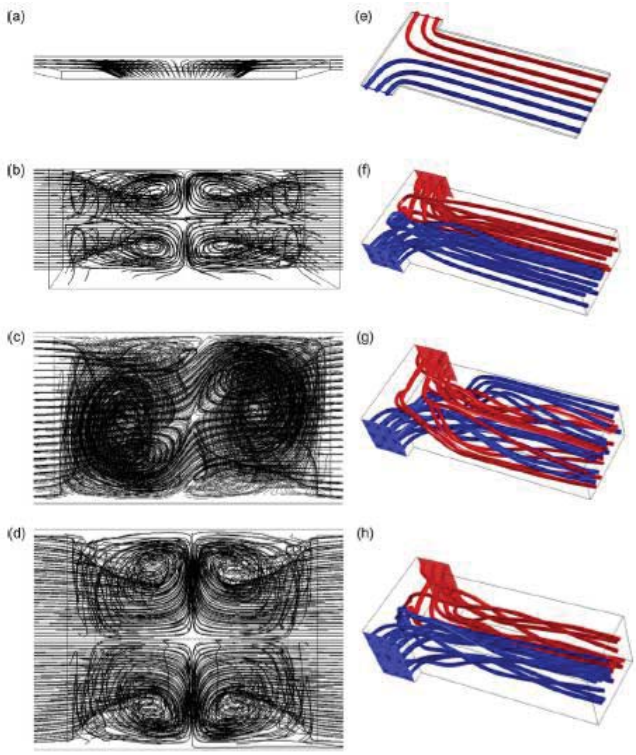

Figure 14. Path lines and streamlines for the aspect ratio of: 0.03 a) and e), 0.42 b) and f), 0.58 c) and g) 0.83 d) and h). Width of the mixing channel is 600 µm: the height of the channel varies according to the aspect ratio.

At low aspect ratio, the flow regime is stratified due to high wall friction and the mixing efficiency is not very high. When the aspect ratio is increased, the flow patterns change and vortices are formed. The numerical simulations revealed an optimum aspect ratio (approx. channel height/channel width = 0.5), where the number of vortices was at its maximum and mixing efficiency was highest. Beyond the optimum aspect ratio, the formation of vortices and the mixing efficiency decreased due to damping of vortices.

3.2.2 Micro T-mixers and experimental procedure

T-mixers and a TT-mixer were constructed based on the numerical simulation results and their mixing efficiency was tested and compared experimentally. The T- and TT-mixers were manufactured by micromachining and PTFE was used as the main construction material. Geometrical information about the T-mixers is presented in Figure 15. The main difference between the T-mixer types was their different aspect ratios.

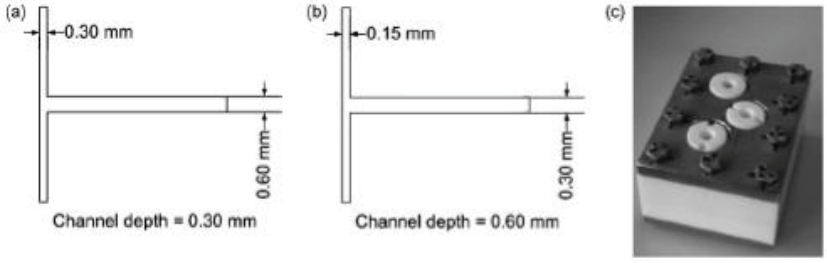

Figure 15. Geometry of T-mixers which were used in the experiments. a) T-mixer(1), b) T-mixer(2). c) housing of the T-mixers.

The main structure and channel dimensions of the TT-mixer are presented in Figure 16. In the TT-mixer, there are two inlets for both components and the components are fed from opposite directions and positions into the mixing channels. In addition, the mixing channel contains circular mixing elements to promote vorticity.

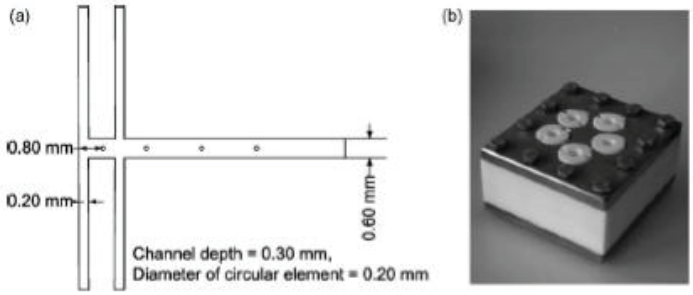

Figure 16. Schematic drawing on the TT-mixer. a) Dimensions of the TT-mixer, b) housing of the TT-mixer.

The performance of the T-type micromixers was compared to a commercial micromixer utilising the multilamination principle. The commercial micromixer used in the comparison was the *Standard Slit Interdigital Micro Mixer* (SSIMM) (Ehrfeld et al., 1999).

3.2.2.1 Test reaction and set-up

There are different methods to study mixing efficiency experimentally. In this study, a method based on the chemical reactions was used. The comparison of mixing efficiency between mixers was carried out by using the fourth Bourne reaction system (Baldyga et al., 1998). This is competition of two parallel reactions:

$$HCl + NaOH \rightarrow NaCl + H_2O, \text{ very fast reaction} \quad (5)$$

$$H_3CC(OCH_3)_2CH_3 + H_2O \xrightarrow{H+} (CH_3)_2CO + 2CH_3OH \quad (6)$$

where $H_3CC(OCH_3)_2CH_3$ is 2,2-dimethoxypropane and $(CH_3)_2CO$ is acetone. Acid catalysed hydrolysis of 2,2-dimethoxypropane (DMP) is carried out parallel with the neutralisation reaction between HCl and NaOH. In the case of extremely rapid and ideal mixing, HCl is neutralised with NaOH that leads to minimal hydrolysis of 2,2-dimethoxypropane. Thus, conversion of the reaction (6) indicates the mixing efficiency: the lower the conversion of the reaction (6) the better the mixing efficiency. A detailed description of the experimental procedure is given in publication IV. A schematic drawing of the experimental set-up is shown in Figure 17.

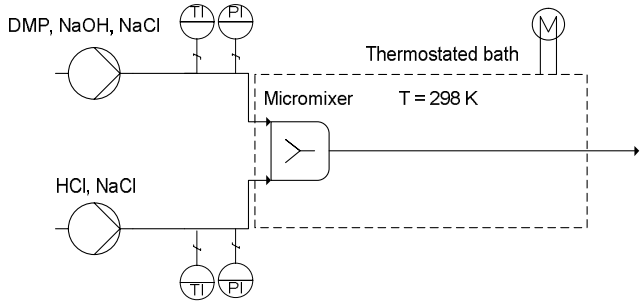

Figure 17. Experimental set-up for mixer testing.

3.2.2.2 Results

Using T-mixer(1) resulted in lower conversion than T-mixer(2). Even though the channel width is longer in T-mixer(1) than in T-mixer(2), T-mixer(1) is a more efficient mixer than T-mixer(2). Geometrical variables have remarkable effects on mixing efficiency. The formation of vortices is greatly dependent on the mixer geometry such as aspect ratio. Vortices essentially enhance mixing efficiency. In the TT-mixer each component has two inlets. In

addition, small circular elements were included in the channel (Figure 16) that accelerated the generation of vortices. By means of this structure, greater contact area could be created between the streams. These features make the TT-mixer a very efficient mixer, as shown in Figure 18 a). The mixing efficiency of the TT-mixer is comparable to the multilamination mixer (*Slit Inderdigital Micro Mixer*). Figure 18 b) illustrates the transition from stratified flow to vortex flow. The mixing efficiency first decreases due to the shortened residence time and then starts to improve due to the vortices, which is characteristic for the transition. The maximum flow rate was 17.8 ml/min corresponding to a Reynolds number of 308.

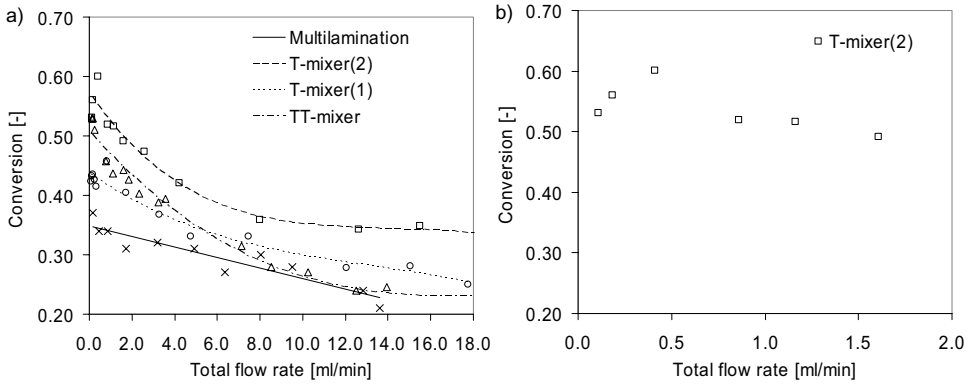

Figure 18. a) Comparison of the micromixers. b) Transition from stratified flow to vortex flow. Lower conversion indicates better mixing efficiency.

3.3 Microseparators

Several applications of microreactors have been presented for chemical reactions (Hessel et al., 2005a), but microprocesses for separation purposes are still rare. In order to get maximum benefits from microprocesses, it is also important to consider downstream processing steps as intensification of the reaction step may merely move the bottleneck to another processing step.

In extraction processes, creation of dispersion by using intensive mixing is rather easy, but separation of immiscible liquids may be a challenge in some cases. In the intensification of extraction processes, efficient separation of liquid phases is an important goal. Benz et al. (2001) demonstrated extraction performance using a micromixer and settler set-up and achieved efficient mass transfer in a micro-scale extraction process. However, the separation of liquid phases took place conventionally by settling. Wengeler et al. (2006) investigated the

potential of a micro hydrocyclone for liquid-liquid separation. The separator utilised the difference in the densities of two liquid phases and showed its potential for liquid-liquid separation. Okubo et al. (2004) presented the performance of a simple microchannel device for coalescing dispersed liquid droplets. The coalescing method is based on the difference in wetting properties of surface materials. The results showed coalescing of liquid droplets in a residence time of less than 1 s.

In this thesis a micro-scale separator for immiscible liquid phases was developed and tested. The separator is called a plate coalescer and utilises the interaction between fluids and solid surfaces in the coalescence of immiscible and dispersed liquid droplets.

3.3.1 Materials and contact angles

In the separation task, organic and aqueous phases were used. The streams were pure water as the aqueous phase and Shellsol D60 with tris(2-ethylhexyl)phosphate (TEHP) as the organic phase. Tris(2-ethylhexyl)phosphate was added into Shellsol to form 10 weight-%, 30 weight-% and 50 weight-% organic solutions. The aqueous and organic phases formed the immiscible mixture.

Solid materials have different surface properties. The surfaces can be classified as high and low energy surfaces depending on how strongly the molecules are bound in the structure. Metal surfaces belong to the group of high energy surfaces and polymer materials to low energy surfaces (Shaw, 1991; Schrader and Loeb, 1992). Solid materials have different interactions with organic and aqueous fluids. The differences in these interactions, in other words the different wetting properties, are utilised in the operation of the plate coalescer.

Contact angle measurements give an indication of the surface properties of solids and measurements were performed to study the interaction between fluids and solid surface. The contact angle is defined as the angle between the baseline of the droplet and the tangent on the boundary of the fluids as shown in Figure 19. The surface is wetted completely if the contact angle is zero. A more detailed description of the measurements is given in publication V.

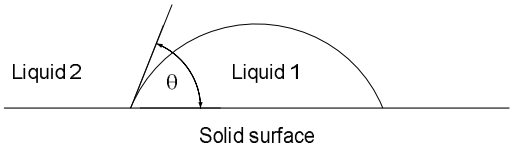

Figure 19. Definition of the contact angle (θ).

The measured contact angles clearly revealed the different wetting properties of the solids. PTFE surface is clearly hydrophobic surface, whereas stainless steel and glass are more hydrophilic. The measured contact angles are presented in Table IV.

TABLE IV Contact angles of water droplets in organic phase on different solid surfaces.

Solid surface	Contact angle (°)
PTFE	160
Stainless steel	102
Glass	87

3.3.2 Plate coalescer

PTFE, stainless steel and glass were selected as the surface materials for the coalescer. The plate coalescer was constructed to enable steady-state continuous phase separation. The main structure of the coalescer contained two plates. A rectangular flat channel was machined on the surface of one of the plates and the channel was located between the plates. The width and length of the coalescer channel were 15 mm and 200 mm, respectively. The height of the channel was either 100 µm or 200 µm. The plate coalescer had one inlet and two outlets. By using reasonable dimensions in the coalescer, the aim was to eliminate high pressure drops and the risk of clogging. Schematic drawings of the experimental system are shown in Figure 20.

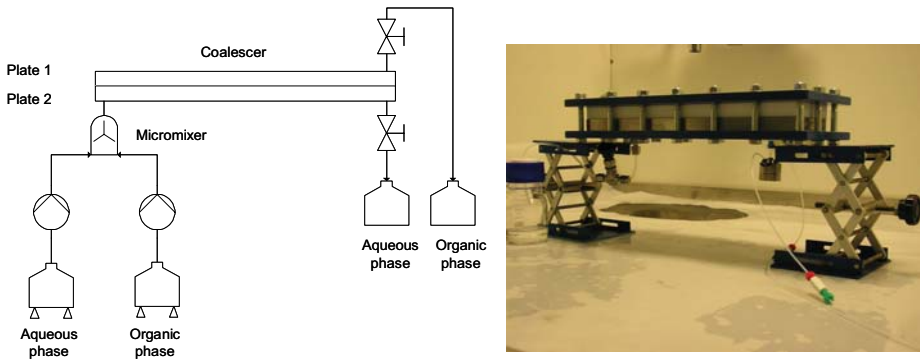

Figure 20. Experimental set-up and scheme of the coalescer.

In the experiments, liquid-liquid dispersion was produced using the *Slit Interdigital Micro Mixer* (Ehrfeld et al., 1999). The liquid-liquid dispersion was then fed immediately into the coalescer, where coalescing of the dispersed droplets started to take place. The separated phases were then withdrawn continuously from their own outlets. The maximum flow rate in the experiments was 480 ml/h, corresponding to a superficial velocity of 8.9 cm/s in the 100 µm height channel and 4.4 cm/s in the 200 µm height channel. The separation efficiency, E, was defined based on the mass fractions of the components, x_i, in the inlet and in the outlet by the following equation:

$$E = 100 \frac{x_{i,INLET} - x_{i,OUTLET}}{x_{i,INLET}} \% \qquad (7)$$

3.3.2.1 Results

Droplet sizes and size distributions are useful information when studying the performance of the coalescer. Droplet diameters in the feed streams before the coalescer were measured as a function of the total flow rate and fluid composition. Droplet size measurements were carried out using a light microscope with image processing software. It was observed that average droplet diameter decreased when the total flow rate was increased and the content of the organic phase also had a minor effect on the average droplet diameter. The dependence of droplet diameter on the total flow rate at different organic phase contents is presented in Figure 21.

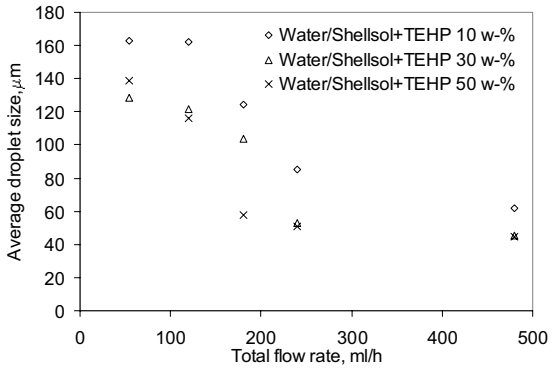

Figure 21. Average droplet diameters before the coalescer as a function of the total flow rates at different compositions of the organic phase. The volumetric flow ratio of the aqueous feed to organic feed was 1:1.

Taking into account the droplet sizes at the beginning of the coalescer, two different cases can be distinguished when interpreting the results. In one case, the average droplet size is larger than the height of the channel and in the other case, the average droplet size is smaller than the height of channel. In the first case (droplet size > channel height), the separation of the liquid phases was complete. The dispersed droplets then have forced contact to the channel surface. This enables the generation of velocity difference between the droplets in the channel due to different wetting properties and further promotes the coalescence and phase separation. In the latter case (droplet size < channel height), separation efficiency was also high. This indicated that the dispersed droplets first collide with each other into larger droplets without forced surface contact. The larger and coalesced droplets then have forced contact to the channel surface, which leads to the velocity difference between the droplets. The smallest droplets reach the larger droplets, which move slower due to the forced surface contact. After reaching the larger droplets, the smaller droplets coalesce into them. The aqueous phase tends to spread on the more hydrophilic surface whereas organic droplets spread on the hydrophobic surface. Both phases could be withdrawn from the coalescer via their own outlets continuously in steady-state. The separation efficiencies as a function of total flow rate at different channel heights are presented in Figure 22.

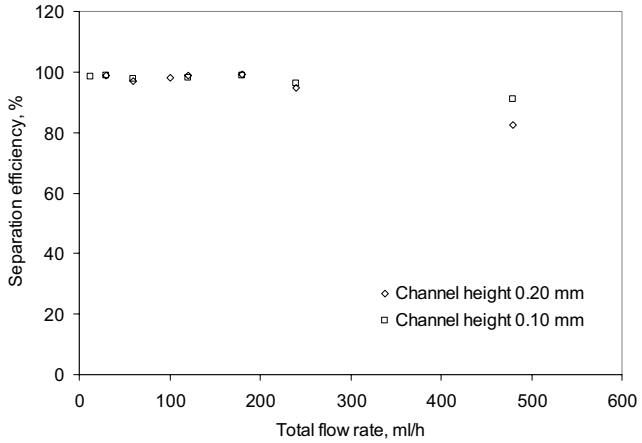

Figure 22. Separation efficiencies as a function of total flow rate.

The difference between channel heights 100 µm and 200 µm could be observed when the separation efficiency was studied as a function of the average flow velocity and the residence time of the liquid-liquid mixture in the coalescer. The coalescer with 100 µm channel enabled

more efficient separation than the coalescer with 200 µm channel when short residence times and higher average flow velocities were used. Separation efficiencies as a function of average flow velocity and residence time at different channel heights are illustrated in Figures 23 and 24.

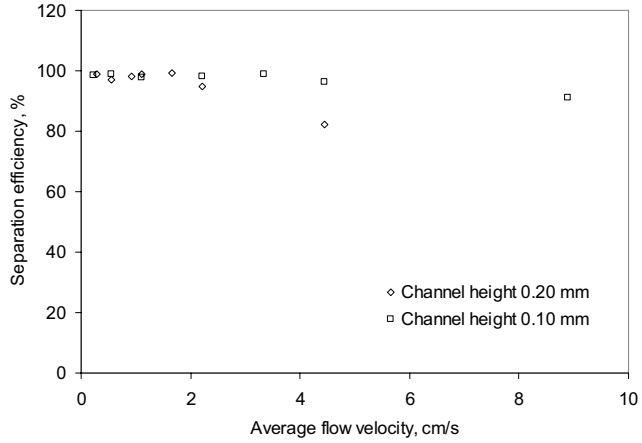

Figure 23. Separation efficiency as a function of average flow velocity.

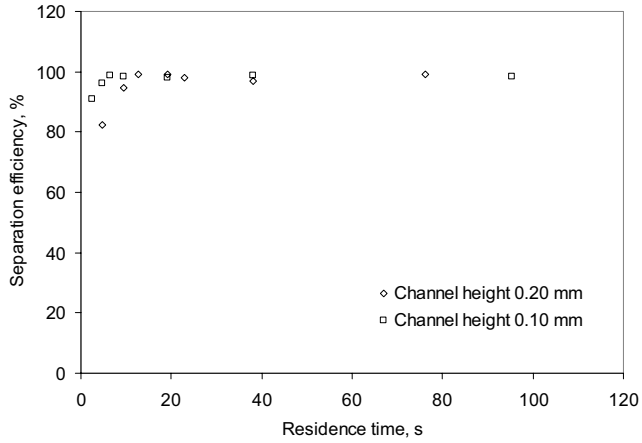

Figure 24. Separation efficiency as a function of residence time.

The role of the surface materials in the phase separation was also under consideration. The combination with PTFE-stainless steel surfaces resulted in the highest separation efficiency under steady-state operation. In the PTFE-stainless steel device, more hydrophilic stainless steel surface exists and water wets it more easily. The behaviour of the PTFE-glass configuration was similar to the PTFE-stainless steel system. The PTFE-PTFE configuration

could not provide continuous steady-state operation in phase separation. Water can neither wet the PTFE channel surface nor spread on it easily. Most of the experiments were carried out with a horizontal plate arrangement. In addition, some experiments were performed by installing the plates in the vertical position. The results did not show significant difference in separation efficiencies between the horizontal and vertical positions.

The concentration of TEHP in Shellsol had no significant influence on the separation efficiency. When the flow rate exceeded 180 ml/h, turbidity started to exist in the aqueous outlet due to small organic droplets (30-60 μm). A flow rate of 180 ml/h corresponds to a superficial velocity of 3.3 cm/s in the 100 μm height channel and 1.7 cm/s in the 200 μm height channel.

In order to evaluate the performance of the plate coalescer, phase separation tests were performed also by settling in a container. The liquid-liquid dispersion with a droplet diameter of 60-120 μm was fed into the container and let separate freely by settling. The time required for the phase separation and disappearance of turbidity was more than 30 min. The plate coalescer was able to decrease the separation time remarkably, having complete separation of less than 20 s in some cases.

For larger scale applications, parallel installation of coalescer units is possible. The number of parallel channels can be decreased by increasing the width of a single channel. Attention should be paid to the height of the channel. Due to the simple structure of the coalescer, manufacturing of a series of coalescer is inexpensive. This aspect can be considered beneficial for feasible scale-up.

4 PROCESS INTENSIFICATION BY FRICTION REDUCTION IN FLUID FLOW

Certain additives reduce frictional pressure drop in pipelines. The phenomenon of friction reduction or drag reduction by additives in turbulent flow offers potential for energy saving and cost reduction in pipelines. These benefits can be interpreted as process intensification.

Usually, high molar mass polymer solutions are used as additives. The additives inducing the drag reduction are often called drag reducing agents (DRA). The drag reducing agents are injected into the pipelines in small amounts. The dosage is usually a few parts per million (ppm). Although, the dosage is small, even 50 % (Al-Wahaibi et al., 2007) and 65 % (Cunha and Andreotti, 2007) frictional reductions can be obtained. The advantages of using drag reducing agents in pipelines are summarised below (Jubran et al. 2005; Manfield et al. 1999):

- Reduction of pressure drop at a certain flow rate
- Increase of flow rate at a certain pressure drop
- Reduction of operating pressure together with reduction of pipe wall thickness
- Reduction of pipe diameter
- Decrease of the number or size of pumping facilities

Polymers which are used in drag reduction can be water soluble or oil soluble. Their molar masses can be of the order of 10^6 g/mol. The polymers are commonly α-olefins and copolymers with high molar mass. Polymethacrylate (PMMA), polyethyleneoxide (PEO) and polyisobutylene (PIB) are examples of drag reducing agents (Jubran et al. 2005).

The drag reduction by additives is achieved in the turbulent flow. After a polymer solution is injected in a pipeline, the polymers elongate due to the shear forces of the turbulent flow. These elongated polymers interact with turbulent eddies. The long chain polymers damp the turbulent eddies when the friction of flow on the pipe wall decreases. The detailed mechanism is not yet fully understood. It has been suggested that polymer elongation plays a key role in drag reduction. Elongation is claimed to occur outside of the viscous sublayer and increase the effective viscosity there leading to damping of turbulent eddies. Other suggestions claim that polymer elasticity and its vibration with turbulence is the dominant mechanism in the drag reduction. It is claimed that polymer chains first stretch in the very near-wall region and

then release in the buffer and log layer. It is proposed that drag reduction is based on the interaction of turbulence characteristics and polymer molecule so that the time scale of turbulence is in relation to the relaxation time of the elongated polymers. In other words, the Kolmogorov time scale should be less than the relaxation time of polymers (Cunha and Andreotti, 2007; Choi and Jhon, 1996; Jubran et al., 2005; Little et al., 1975).

The strength of the drag reduction is often described by the percentage drag reduction effect, the DR-effect. In pipe flow, the DR-effect can be obtained by measuring pressure drops with and without drag reducing agent using the following expression (Manfield et al., 1999):

$$DR-\% = 100\% \frac{\Delta p_0 - \Delta p_{DRA}}{\Delta p_0} \tag{8}$$

The drag reduction effect can be determined also in a rotating apparatus. In the rotating apparatus, there is a plate or cylinder rotating inside a vessel, which is filled with liquid. The DR-effect can be obtained by measuring the torque with and without drag reducing agent and using the following equation (Choi and Jhon, 1996):

$$DR-\% = 100\% \frac{T_0 - T_{DRA}}{T_0} \tag{9}$$

The following characters have been observed experimentally and the following conclusions can be drawn from literature:

- Turbulence is required for the phenomena
- The higher the molar mass of the drag reducing agent, the stronger the DR-effect
- The higher the dosage of drag reducing polymer, the stronger the DR-effect

The drag reduction effect decreases during operation due to degradation of the polymers. Shear forces in the turbulent flow cause the scission of the polymer chain, which leads to a decrease in the DR-effect. Since the DR-effect is proportional to the molar mass of the polymer, the following principle for the correlation of the degradation effect has been proposed (Brostow et al., 1990):

$$\frac{DR-\%(t)}{DR-\%_0} = \frac{M(t)}{M_0} \tag{10}$$

In Equation (10), DR-$\%_0$ and M_0 denote the initial DR-effect and molar mass of the polymer, respectively. The affecting molar mass of the polymers, M(t), determines the DR-effect at time t.

4.1 Drag reduction effects of oil-soluble polymers

In this thesis, the efficiency of the DR-effect was studied in different flow conditions. A wide range of apparent molar masses of drag reducing polymers was used in the experiments. The decay of the DR-effect was also under consideration.

4.1.1 Materials and set-up

The experiments were carried out in a rotating device. The device consisted of a vessel, which was equipped with a rotating cylinder. The vessel was filled with bulk liquid, which was diesel oil. The rotation speed of the cylinder could be varied in the range of 0-3200 1/min, corresponding to a Reynolds number range 0-262 000. The Reynolds number for a rotating device is defined by means of rotation speed, cylinder diameter and kinematic viscosity:

$$\mathrm{Re} = \frac{nD^2}{\nu} \tag{11}$$

The torque was measured in the experiments for the determination of the DR-effect. Other details of the apparatus are given in publication VI. A drawing of the measurement apparatus is shown in Figure 25.

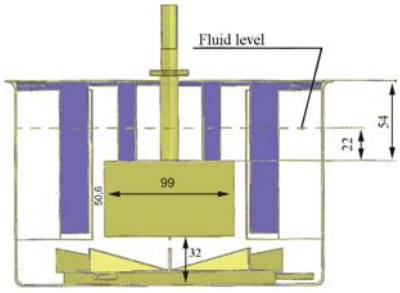

Figure 25. Measurement apparatus for the drag reduction effect.

Mainly hexene and small concentrations of comonomers decene and dodecene were used in the polymerisation of the drag reducing polymers. The polymers were dissolved in a hydrocarbon solution. In the experiments, apparent molar masses of the polymers were varied from $1 \cdot 10^6$ g/mol to $31 \cdot 10^6$ g/mol. A certain amount of polymer solution was injected in the bulk liquid at the beginning of the experiment in order to get the desired concentration of the polymer in the bulk liquid. The concentration of a polymer in the bulk liquid was varied from 1.3 w-ppm to 9.3 w-ppm.

4.1.1.1 Results

The results revealed that the maximum DR-effect in the experiment was approximately 40 %. Generally, increasing the polymer concentration in the bulk liquid, molar mass and rotation speed enhanced the DR-effect, as can be seen in Figures 26-28. A clear improvement in the DR-effect could be observed when the apparent molar mass of polymer approaches the value $5 \cdot 10^6$ g/mol. This indicates the onset of the phenomenon in terms of molar mass.

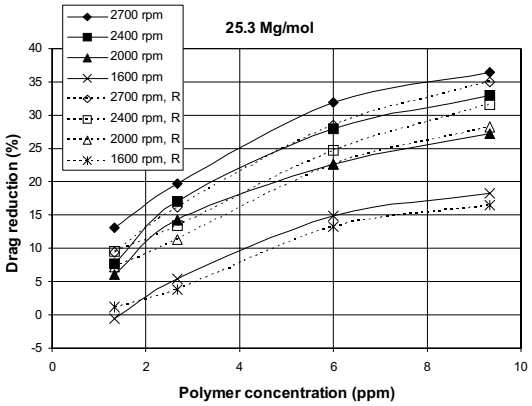

Figure 26. Effect of polymer concentration on the DR-effect at different rotation speeds. The label "R" means a repetition of a measurement.

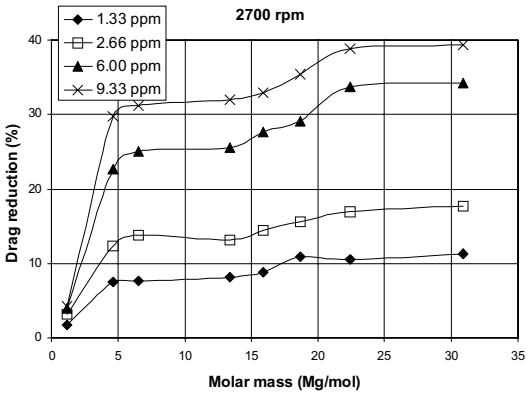

Figure 27. Effect of apparent polymer molar mass on the DR-effect at different polymer concentrations.

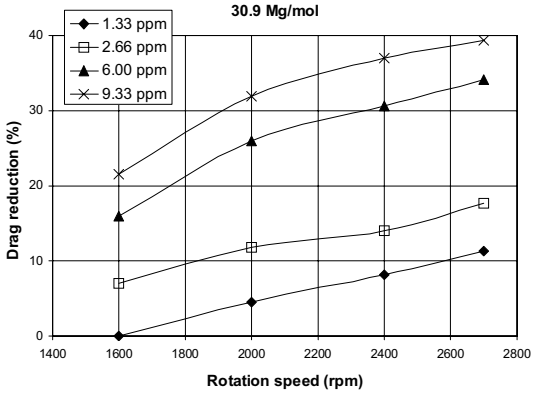

Figure 28. Effect of rotation speed on the DR-effect at different polymer concentrations. Rotation speed can be converted to Reynolds number.

To derive a correlation for the measured DR-effect, the strength of the DR-effect was separated into three factors: the effect of molar mass, polymer concentration, and flow conditions. The product of the factors (activity functions $\gamma_1(C)$, $\gamma_2(M)$ and $\gamma_3(Re)$) describes the ratio of the DR-effect to the maximum DR-effect as shown in Equation (12).

$$\frac{DR-\%}{DR_{\max}} = \gamma_1(C)\cdot\gamma_2(M)\cdot\gamma_3(\mathrm{Re}) \tag{12}$$

In this approach, each activity function $\gamma_1(C)$, $\gamma_2(M)$ and $\gamma_3(Re)$ describes how strong influence the factors C, M and Re have on the DR-effect. Suitable activity function forms are extracted from experimental data by setting $\gamma_i = 1.0$ for maximum C, M and Re. The single γ_i -activity function describes the ratio of DR-%/$DR_{\max}$ with respect to the factor in question. The fitted activity functions with respect to concentration, molar mass and Reynolds number are shown in Figures 29-31.

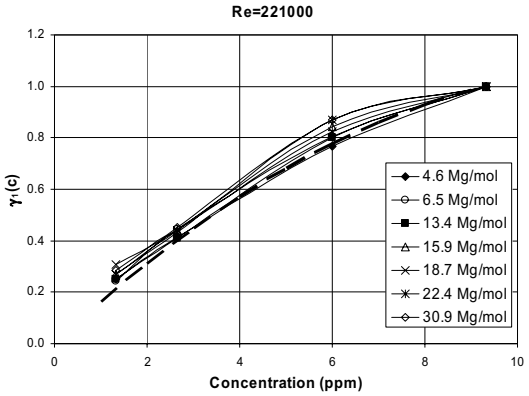

Figure 29. Measured activity of concentration. Dashed line indicates the fitted activity function $\gamma_1(C)$.

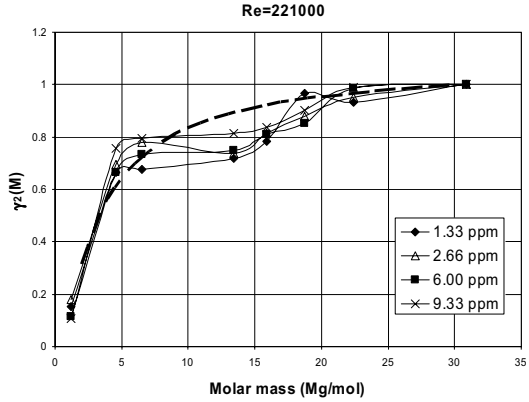

Figure 30. Measured activity of molar mass. Dashed line indicates the fitted activity function $\gamma_2(M)$.

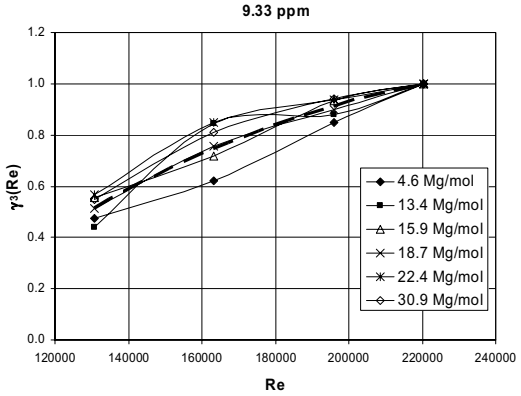

Figure 31. Measured activity of Reynolds number. Dashed line indicates the fitted activity function $\gamma_3(\mathrm{Re})$.

The experiments revealed that the DR-effect decreased during the operation. This was due to breaking of the polymers. At rotation speed higher than 3100 1/min (Re = 254 000) polymers degradaded immediately. Shear forces in the flow break the polymer chain into smaller chains. Even though the polymer chains are broken, they still have the ability to reduce drag. It was also observed that degradation kinetics depends on the initial polymer molar mass, Reynolds number and operation time. The degradation experiments were performed for a wide variety of polymers. Modelling of degradation kinetics is based on the apparent molar mass (M) of the polymers. The apparent and final molar mass (M_f) were determined from the DR-effect information. Taking into account the initial molar mass (M_0) and time constant for decay (τ), the apparent molar mass is then expressed as follows:

$$M = \left(M_0 - M_f\right)e^{-t/\tau} + M_f \qquad (13)$$

Time constant, τ, characterises here the decay of the polymer only in the above mentioned type of device, which was a rotating device. In pipe flow, a re-determination of time constant is needed due to different flow patterns. Details on determining the time constant are explained in publication VI. Figure 32 shows the experimental and modelled DR-effect as a function of time when polymer degradation is taken into account.

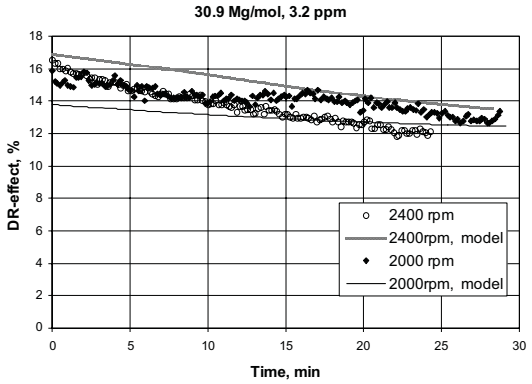

Figure 32. DR-effect and degradation of the drag reducing polymer. Experimental results and modelled degradation when initial molar mass of drag reducing polymer is $30.9 \cdot 10^6$g/mol and dosage 3.2 ppm.

As can be seen from Figure 32, there is some deviation between the experimental and modelled DR-effects. The phenomena in question are rather complicated. In this study, the characterisation of polymers is based on the apparent molar mass. However, better characterisation would contain also molar mass distribution and relaxation properties of polymers. The interaction of polymer characteristics and turbulence phenomena in different spaces play a significant role and doubtless affect the drag reducing phenomena. These aspects make detailed and exact modelling very challenging. However, derived correlations can be used for developing CFD models to describe hydrodynamics in fluid flow when drag reducing agents are used.

5 ECONOMIC BENEFITS FROM PROCESS INTENSIFICATION

Opportunities for process intensification exist when there is a need to reduce energy consumption, produce less waste, improve safety, improve product quality, shorten residence time or improve yield. Process intensification enables the change from a batch process to a continuous process, leading to cost savings on a plant level (Green et al., 1999).

In this chapter, batch and continuous processes are compared economically. In the evaluation of batch operation, tank reactors are under consideration and the economical comparison is based on an example reaction. In tank reactors, operation may be limited by heat or mass transfer resulting in increased residence time. Uneven temperatures and concentrations in the reactor and long residence time favour the formation of by-products and impurities. Cleaning and washing operations between batches are time-demanding and frequent cleaning produces large amounts of wastes. Continuous and intensified processes enable operation in more optimal conditions than batch processes and stirred tank reactors. More optimal conditions mean better reaction performance in terms of higher conversion and selectivity, with less formation of impurities and fewer unwanted by-products. High heat transfer efficiency eliminates possible thermal hot-spots and may reduce the residence time of the process. There is no need to control heat formation by the feed rate of a reactant. High heat transfer capacity may also eliminate extra solvents, which previously have been used as thermal mass. Savings in raw material and waste costs are then possible.

The cost structures of batch and continuous processes are compared in this study. A step of a production process for a fine chemical is used as a reaction example. Some information about the process and the detailed cost structure of batch and continuous processes is given in publication VII. In the case studied, the difference between batch and continuous processing originates from the costs of raw material and waste as well as investment cost. In this case, the profit difference between the continuous and batch process can be described by Equation 14.

$$Y_2 - Y_1 = 0.4R + 0.5W_2 + \frac{P(t_1 - t_2)}{m_1} - \frac{0.25I}{M} \qquad (14)$$

Equation (14) takes into account raw material costs (R), waste cost (W_2), production costs (P), residence time in batch (t_1) and continuous processing (t_2), batch size (m_1), investment costs (I) and total production amount (M) during production period. Due to more optimal conditions in the continuous and intensified process, savings in raw material and waste costs are assumed. In addition, investment costs are assumed higher for the continuous process than the batch process. In Equation (14), the factor 0.4 indicates 40 % savings in raw material costs and 0.5 indicates 50 % savings in waste costs. The factor, 0.25 indicates 25 % higher investment costs in the case of the continuous process.

A significant influence on cost structure is seen when the residence time decreases. If the residence time of the batch process (t_1) decreases from 30 hours to 25, 20 and 15 hours (t_2) of the intensified process, effects on profit difference are the higher the higher the production cost (manpower, utilities, etc.) is. This is demonstrated in Figure 33. The main effect originates from the increased production capacity, which decreases the relative production cost (€/kg) significantly. The costs and profits are calculated based on the kilogram of product. However, it should be remembered that in a multi-stage process the bottleneck of the process may move elsewhere. The effect of production cost on the profit difference between continuous and batch processes is shown in Figure 33 at the residence times of 15, 20 and 25 hours. The residence time of the batch process is 30 hours. The residence times 15, 20 and 25 hours refer to the intensified process.

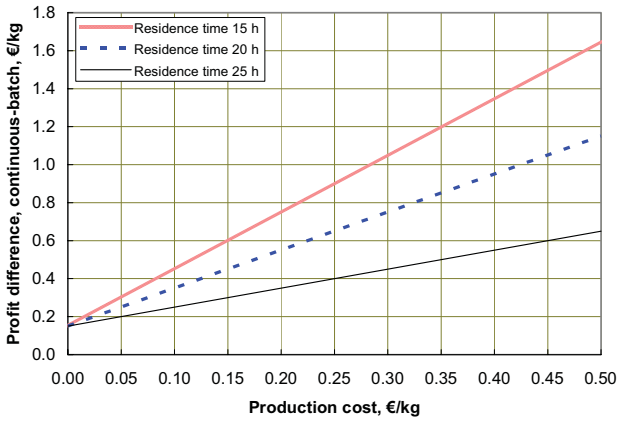

Figure 33. Effect of production cost on profit difference between the continuous and batch process at different residence times. The residence time of the batch process is 30 hours. The residence times 15, 20 and 25 hours refer to the intensified process.

An essential aspect is that the time saving in production period enables new production (or product) on the same production line. This increases the company profit further.

6 CONCLUSIONS

Process intensification is one of the most popular trends in chemical engineering. It has mainly focused on reactor technology with reactions, heat and mass transfer operations.

Process intensification enables operation often in more optimal conditions, where better yields, shorter residence time, raw material savings, and smaller amounts of waste are possible. This clearly has a beneficial effect on the production economics.

Separation stages also offer potential for process intensification. In a production process, intensification of reaction steps may move the rate limiting step to another processing stage. It is, therefore, essential to consider also separation tasks in process intensification.

Microreactors represent process intensification as its extreme. The high ratio of surface area to volume is an important feature in microchannels. It evidently enhances heat and mass transfer. In addition, this feature can be utilised in separation stages because interaction between surface materials and fluids becomes important. Hydrophilic and hydrophobic materials which are in the contact with fluids have effects on hydrodynamics. In certain cases, such as in coalescing of immiscible liquid droplets, the interaction can be utilised. Coalescing of liquid droplets in the plate coalescer can be applied effectively in the separation of immiscible liquid phases, as shown in this thesis.

In microscale channels, phenomena may be different than in large scale channels and empirical correlations derived for large scale channels may not be totally valid for microchannels. Therefore, it is important to study phenomena in microchannels carefully. For example, convective phenomena enhance mixing essentially in microchannels, although the low Reynolds number clearly indicates laminar flow. This finding is shown in this thesis in the context of micro T-mixers.

During the life cycle of a process, fast transfer of laboratory research results to the production stage gives economical benefits with respect to competitors. In microreactor technology, process development is assumed to be performed by the numbering-up principle. As a

principle, it is fast, straightforward, and eliminates errors originating from scale difference. Numbering-up does, however, have some disadvantages. In the case of many parallel channels, equal fluid distribution is difficult to achieve. It is also an expensive approach: manufacturing of a high number of channels is expensive and time consuming.

Process development in microreactor technology can be accelerated if the structure of a repeatable process unit is rather simple and the dimensions can be kept to a reasonable level. These aspects make process development even by numbering-up more feasible. When designing microstructured components, special attention has to be paid to avoiding their main disadvantages. Typical problems of microreactors are clogging, fluid distribution problems, and difficulties in monitoring of the process. The micro T-mixers and plate coalescer presented in this thesis proved to be simple and efficient devices. Monolith reactors represent the concept of a multichannel and small-scale channel device, which can operate reliably without clogging, and where an even fluid distribution can be achieved.

In the field of process intensification, innovations are needed when combining materials, structures, hydrodynamics and their interactions to design and intensify process units.

7 REFERENCES

Al-Wahaibi, T., Smith, M., Angeli, P. (2007). Effect of drag-reducing polymers on horizontal oil-water flows, *Journal of Petroleum Science and Engineering*, **57**, pp. 334-346.

Baldyga, B., Bourne, J.R., Walker, B. (1998). Non-isothermal Micromixing in Turbulent Liquids: Theory and Experiment, *The Canadian Journal of Chemical Engineering*, **76**, pp. 641-649.

Bakker, R.A., Stankiewicz, A., Schyns, V.J.A.J. (2001). Process intensification within DSM, general methodology and concrete examples, Better Processes for Better Products, 4th International Conference on Process Intensification for the Chemical Industry, pp. 33-45.

Bayer, T., Himmler, K., Hessel, V. (2003). Don't be baffled by static mixers, *Chem. Eng.*, **5**, pp. 2-9.

Benz, K., Jäckel, K.-P., Regenauer, K.-J., Schiewe, J., Drese, K., Ehrfeld, W., Hessel, V., Löwe, H. (2001). Utilization of Micromixers for Extraction Processes, *Chemical Engineering & Technology,* 24, pp. 11-17.

Bercic, G., Pintar, A. (1997). The role of gas bubbles and liquid slug lengths on mass transport in the Taylor flow through capillaries, *Chemical Engineering Science*, 52, pp. 3709-3719.

Bothe, D., Stemich C., Warnecke, H.-J. (2006). Fluid mixing in a T-shaped micro-mixer, *Chemical Engineering Science*, **61**, pp. 2950-2958.

Broekhuis, R.R., Machado, R.M., Nordquist, A.F. (2001). The ejector-driven monolith loop reactor – experiments and modeling, *Catalysis Today*, **69**, pp. 87-93.

Brostow, Witold., Ertepinar, H., Singh, R.P. (1990). Flow of Dilute Polymer Solutions: Chain Conformations and Degradation of Drag Reducers, *Macromolecules*, **23**, pp. 5109-5118.

Choi, H.J., Jhon, M.S. (1996). Polymer-Induced Drag Reduction, *Ind. Eng. Chem. Res.*, **35**, pp. 2993-2998.

Crynes, L.L, Cerro, R.L., Abraham, M.A. (1995). Monolith Froth Reactor: Development of a Novel Three-Phase Catalytic System, *AIChE Journal*, **41**, pp. 337-345.

Cunha, F.R., Andreotti, M. (2007). A Study of the Effect of Polymer Solution in Promoting Friction Reduction in Turbulent Channel Flow, *Journal of Fluids Engineering*, **129**, pp. 491-505.

Edvinsson, R.K, Cybulski, A. (1995). A comparison between the monolithic reactor and the trickle-bed reactor for the liquid-phase hydrogenations, *Catalysis Today*, **24**, pp. 173-179.

Engler, M., Kockmann, N., Kiefer, T., Woias, P. (2004). Numerical and experimental investigations on liquid mixing in static micromixers, *Chemical Engineering Journal*, **101**, pp. 315-322.

Ehrfeld, W., Golbig, K., Hessel, V., Löwe, H., Richter, T. (1999). Characterization of mixing in Micromixers by a Test Reaction: Single Mixing Units and Mixer Arrays, *Ind. Eng. Chem. Res*., **38**, pp. 1075-1082.

Gladden, L.F., Lim, M.H.M., Mantle, M.D., Sederman, A.J., Stitt, E.H. (2003). MRI visualisation of two-phase flow in structured supports and trickle-bed reactors, *Catalysis Today*, **79-80**, pp. 203-210.

Green, A. (1998). Process Intensification: the key to survival in global markets?, *Chemistry & Industry*, pp. 168-172.

Green, A., Johnson, B., Arwyn, J. (1999). Process Intensification Magnifies Profits, *Chemical Engineering*, **106**, pp. 66-73.

Haakana, T., Kolehmainen, E., Turunen, I., Mikkola, J-P., Salmi, T. (2004). The development of monolith reactors: general strategy with a case study, *Chemical Engineering Science*, **59**, 24, pp. 5629-5635.

Haario, H. (1994). *ModEst User Manual*, Profmath Oy, Helsinki.

Heibel, A.K., Scheenen, T.W.J., Heiszwolf, J.J., Van As, H., Kapteijn F., Moulijn, J.A. (2001). Gas and liquid phase distribution and their effect on reactor performance in the monolith film flow reactor, *Chemical Engineering Science*, **56**, pp. 5935-5944.

Hessel, V., Hardt, S., Löwe H. (2004). *Chemical Micro Process Engineering, -Fundamentals, Modelling and Reactions*, Wiley-VCH GmbH & Co, Weinheim.

Hessel, V., Löwe H., Müller, A., Kolb, G. (2005a). *Chemical Micro Process Engineering, -Processing and Plants*, Wiley-VCH GmbH & Co, Weinheim.

Hessel, V., Hardt, S., Löwe, H., Schönfeld, F. (2003). Laminar Mixing in Different Interdigital Micromixers: I. Experimental Characterization, *AIChE Journal*, **49**, pp. 566-577.

Hessel, V., Löwe, H., Schönfeld, F. (2005b). Micromixers – a review on passive and active mixing principles, *Chemical Engineering Science*, **60**, pp. 2479-2501.

Hoffmann, M., Schlüter, M., Räbiger, N. (2006). Experimental investigation of liquid-liquid mixing in T-shaped micro-mixers using μ-LIF and μ-PIF, *Chemical Engineering Science*, **61**, pp. 2968-2976.

Irandoust, S., Andersson, B., Bengtsson, E., Siverström, M. (1989). Scaling Up of a Monolithic Catalyst Reactor with Two-Phase Flow, *Ind. Eng. Chem. Res*., **28**, pp. 1489-1493.

Jubran, B.A., Zurigat, Y.H., Goosen, M.F.A. (2005). Drag Reducing Agents in Multiphase Flow Pipelines: Recent Trends and Future Needs, *Petroleum Science and Technology*, **23**, pp. 1403-1424.

Kim, C.A., Kim, J.T., Lee, K., Choi, H.J., Jhon, M.S. (2000). Mechanical degradation of dilute polymer solution under turbulent flow, *Polymer*, **41**, pp. 7611-7615.

Kolehmainen, E., Turunen, I. (2007). Micro-Scale Liquid-Liquid Separation in a Plate-Type Coalescer, *Chemical Engineering and Processing*, **46**, pp. 834-839.

Koskinen, J., Manninen, M., Pättikangas, T., Alopaeus, V., Keskinen, K.I., Kolehmainen, E. (2004). Measurements and CFD modeling of drag-reduction effects, *SPE Production & Facilities*, **19**, 142-151.

Kresta, S.M., Krebs, R., Martin, T. (2004). The Future of Mixing Research, *Chemical Engineering & Technology*, 27, pp. 208-214.

Kreutzer, M.T., Du, P., Heiszwolf, J.J., Kapteijn, F., Moulijn, J.A. (2001). Mass transfer characteristics of three-phase monolith reactor, *Chemical Engineering Science*, **56**, pp. 6015-6023.

Little, R.C., Hansen, R.J., Hunston, D.L., Kim., O.-K., Patterson, R.L., Ting, R.Y. (1975). The drag reduction Phenomenon. Observed Characteristics, Improved Agents, and Proposed Mechanisms, *Ind. Eng. Chem. Fundam.*, **14**, pp. 283-296.

Manfield, P.D., Lawrence, C.J., Hewitt, G.F. (1999). Drag reduction with additives in multiphase flow: a literature review, *Multiphase Science and Technology*, **11**, 197-221.

Mantle, M.D., Sederman, A.J. (2003). Dynamic MRI in chemical process and reaction engineering, *Progress in Nuclear Magnetic Resonance Spectroscopy*, **43**, pp. 3-60.

Okubo, Y., Toma, M., Ueda, H., Maki, T., Mae, K. (2004). Microchannel devices for the coalescence of dispersed droplets produced for use in rapid extraction processes, *Chemical Engineering Journal*, **101**, pp. 39-48.

Ramshaw, C. (1983). "HIGEE" Distillation – An example of Process Intensification, *The Chemical Engineer*, pp. 13-14.

Reinecke, N., Mewes, D. (1996). Tomographic imaging of trickle-bed reactors, *Chemical Engineering Science*, **51**, pp. 2131-2138.

Reinecke, N., Mewes, D. (1997). Investigations of the two-phase flow in trickle-bed reactors using capacitance tomography, *Chemical Engineering Science*, **52**, pp. 2111-2127.

Reinecke, N., Petritsch, G., Boddem, M., Mewes, D. (1998). Tomographic imaging of the phase distribution in two-phase slug flow, *Int. J. Multiphase Flow*, **24**, pp. 617-634.

Roy, S., Bauer, T., Al-Dahnan, M., Lehner, P., Turek, T. (2004). Monoliths as Multiphase Reactors: A Review, *AIChE Journal*, **50**, pp. 2918-2938.